Thermoelectricity and thermodiffusion in charged colloids

B. T. Huang, M. Roger, M. Bonetti, T. J. Salez, C. Wiertel-Gasquet, Emeric
Dubois, R. Cabreira Gomes, G. Demouchy, G. Mériguet, V. Peyre, et al.

Thermoelectricity and thermodiffusion in charged colloids

B. T. Huang, M. Roger, M. Bonetti, T. J. Salez, C. Wiertel-Gasquet, E. Dubois, R. Cabreira Gomes, G. Demouchy, G. Mériguet, V. Peyre, M. Kouyaté, C. L. Filomeno, J. Depeyrot, F. A. Tourinho, R. Perzynski, and S. Nakamae

Articles you may be interested in

Thermodiffusion in concentrated ferrofluids: A review and current experimental and numerical results on non-magnetic thermodiffusion
Phys. Fluids **25**, 122002 (2013); 10.1063/1.4848656

Collective thermodiffusion of colloidal suspensions
J. Chem. Phys. **137**, 194904 (2012); 10.1063/1.4767398

Thermal diffusion behavior of hard-sphere suspensions
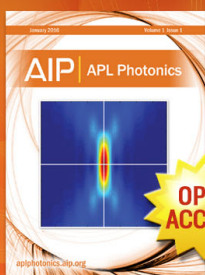J. Chem. Phys. **125**, 204911 (2006); 10.1063/1.2400860

Negative thermodiffusion of polymers and colloids in solvent mixtures
J. Chem. Phys. **118**, 8073 (2003); 10.1063/1.1563601

Phase separation in suspensions of colloids, polymers and nanoparticles: Role of solvent quality, physical mesh, and nonlocal entropic repulsion
J. Chem. Phys. **118**, 3880 (2003); 10.1063/1.1538600

Thermoelectricity and thermodiffusion in charged colloids

B. T. Huang,[1] M. Roger,[1] M. Bonetti,[1] T. J. Salez,[1,2] C. Wiertel-Gasquet,[1] E. Dubois,[3] R. Cabreira Gomes,[3,4] G. Demouchy,[3,5] G. Mériguet,[3] V. Peyre,[3] M. Kouyaté,[3] C. L. Filomeno,[3,4] J. Depeyrot,[4] F. A. Tourinho,[4] R. Perzynski,[3] and S. Nakamae[1,a]

[1]*Service de Physique de l'Etat Condensé, CEA-IRAMIS-SPEC, CNRS, UMR 3680, CEA Saclay, F-91191 Gif-sur-Yvette Cedex, France*
[2]*École des Ponts ParisTech, 6 et 8 Avenue Blaise Pascal, Champs-sur-Marne, F-77455 Marne-la-Vallée, France*
[3]*Sorbonne Universités, UPMC Univ Paris 06, CNRS, Laboratoire PHENIX, Case 51, 4 Place Jussieu, F-75005 Paris, France*
[4]*Grupo de Fluidos Complexos, Instituto de Fisica & Instituto de Quimica, Universidade de Brasília, CP 04478, 70904-970 Brasília (DF), Brazil*
[5]*Université Cergy-Pontoise, Département de la Physique, 33 Bd du Port, F-95011 Cergy-Pontoise Cedex, France*

The Seebeck and Soret coefficients of ionically stabilized suspension of maghemite nanoparticles in dimethyl sulfoxide are experimentally studied as a function of nanoparticle volume fraction. In the presence of a temperature gradient, the charged colloidal nanoparticles experience both thermal drift due to their interactions with the solvent and electric forces proportional to the internal thermoelectric field. The resulting thermodiffusion of nanoparticles is observed through forced Rayleigh scattering measurements, while the thermoelectric field is accessed through voltage measurements in a thermocell. Both techniques provide independent estimates of nanoparticle's entropy of transfer as high as 82 meV K^{-1}. Such a property may be used to improve the thermoelectric coefficients in liquid thermocells. © *2015 AIP Publishing LLC.* [http://dx.doi.org/10.1063/1.4927665]

I. INTRODUCTION

In solid thermoelectric materials, if a temperature gradient is applied to a conductor, the electrons in contact with the hot part acquire a kinetic energy and diffuse to the cold side. This leads to the buildup of an internal electric field, which is proportional to the temperature gradient, known as Seebeck effect. In charged colloidal suspensions, the migration of charged species is also induced by the presence of a thermal gradient, which is known as thermodiffusion or thermophoresis. These charged species act as charge carriers, analogous to electrons in solids. The resulting thermoelectric effect with contributions coming from both electrolytes and charged colloidal particles themselves is known to influence the thermodiffusion behavior of charged colloidal suspensions.[1,2] The thermoelectric effect (Seebeck effect) is known to influence the thermodiffusion behavior of charged colloidal suspensions with contributions coming from both electrolytes and charged colloidal particles themselves.[1–3] Under a thermal gradient $\boldsymbol{\nabla}T$, the thermal drift of ionic species, i, induces concentration gradients $\boldsymbol{\nabla}n_i/n_i = -\alpha_i\boldsymbol{\nabla}T$ (Soret effect) and an internal electric field $\boldsymbol{E} = \mathcal{S}_e\boldsymbol{\nabla}T$ (Seebeck effect). Both Soret (α_i) and Seebeck ($\mathcal{S}_e$) coefficients depend on the *Eastman entropies of transfer* $\widehat{S}_i$,[2–6] which characterize the interaction of species i with the surrounding ions and molecules.[7] The absolute value of $\widehat{S}_i$ generally increases with the ion size. Large Soret effects have indeed been reported experimentally in various colloidal suspensions such as silica particles, DNA molecules, polystyrene spheres, and magnetic nanoparticles

(NPs) (ferrofluids)[8–13] reflecting the large Eastman entropy of transfer associated with their equally large physical size (in the nm–μm range). On the other hand, direct measurements of thermoelectric voltage in charged colloidal suspensions have rarely been reported.[14]

Here, we investigate one such charged colloidal suspension, namely, ionically stabilized ferrofluid in dimethyl sulfoxide (DMSO). Ferrofluid was chosen not only because of the high Soret coefficients[13,15] of NPs among other colloidal suspensions with nanometric particle size but also because of their magnetic nature which may offer an additional parameter (magnetic field[16,17]) to control the thermoelectric property of colloidal suspensions. We determine independently the Eastman entropy of transfer of NPs $\widehat{S}$ through (i) the Soret effect using forced Rayleigh scattering measurements and (ii) the Seebeck effect using a thermocell (see Sec. II). The values of $\widehat{S}$ deduced from the two experiments agree quantitatively and are almost three orders of magnitude higher than those of typical ions in electrolytes.[4] Furthermore, we show that the thermodiffusion of NPs has a sizable influence on the Seebeck coefficient, an effect that may be used in liquid thermoelectric applications.[18]

II. EXPERIMENTAL SECTION

A. Samples

We have used ferrofluids based on well-known maghemite γ-Fe$_2$O$_3$ nanoparticles dispersed in DMSO. Our prior investigations on several liquids (water, organic solvents, alcohol, and ionic liquids) revealed the Seebeck coefficient of pure

a)Electronic mail: sawako.nakamae@cea.fr

DMSO to be negligible, making it suitable for studying the thermoelectric voltage dependence on the NP concentration. The median NP diameter of $d = 6.7$ nm and the polydispersity 0.38 of the log-normal size distribution are determined from room-temperature magnetization measurements on a dilute ferrofluid sample.[19] Nanoparticles are chemically synthesized first in water (see Ref. 20 for methods). This dispersion gives a ferrofluid of positively charged NPs with nitrate counterions, which are then replaced by perchlorate ones to ensure the NPs colloidal stability in DMSO following the method described in Ref. 21. DMSO is added instead of water at the end of the process to obtain electrostatically stabilized dispersion with positively charged NP surface. The concentration of free perchloric acid in the subsequent solutions (obtained via dilution) was kept constant at ≈ 12.5 mM. This value was determined from the conductivity measurement in the supernatant of DMSO ferrofluid obtained after ultracentrifugation (60 000 rpm, 1h30) which separates the NPs from the solvent.

B. Thermodiffusion measurements

The forced Rayleigh scattering technique used to extract the Soret and the NPs diffusion coefficients is well described in the work of Demouchy *et al.*[22] The heating light (Hg arc lamp, 100 Hz modulation) creates the optical image of a grid in the sample. Owing to the optical absorption by the NPs, a temperature grating is induced in the sample. Then, a NP concentration grating settles due to the Soret effect in a few seconds at the spatial scale of ≈ 50 μm. Both gratings are detected by the diffraction of a weakly absorbing test laser beam. As the gratings of the temperature and the NPs concentration evolve on time scales differing by orders of magnitude, this technique enables the use of a "*two-time scale*" model.[22] The Soret coefficient is deduced from the temporal modulation of scattered intensity at constant spatial modulation of NPs concentration. The diffusion coefficient D is determined by the relaxation time measurement of the concentration grating after the heating source is switched off at different spatial modulations.[23]

C. Thermoelectric measurements

The Seebeck coefficient measurements were performed in a homemade thermocell consisting of a vertical, cylindrical Teflon cell (14 mm high and 6 mm diameter) with two ends sealed by sapphire windows, similar to the setup described in Refs. 24 and 25. The ferrocene/ferrocenium (F_C/F_C^+) redox couple (2/4 mM, respectively) was added to the sample in order to permit the exchange of electrons between the electrodes and the ferrofluid. These chemicals were purchased from *Sigma Aldrich*; ferrocene (F_C, 98%) and ferrocenium-tetrafluoroborate ($F_C BF_4$, technical grade) are used as received. The sample preparation is performed in a glovebox under a nitrogen atmosphere. It should be noted that the co-existence of the redox couple and nanoparticles did not change the redox potential (cf. the supplementary material (Sec. I)[39]) or cause aggregation of NPs. The experiments are carried out with the temperature difference between the two electrodes $\Delta T_{elect} \approx 4.3$ °C (10 °C difference between the cell
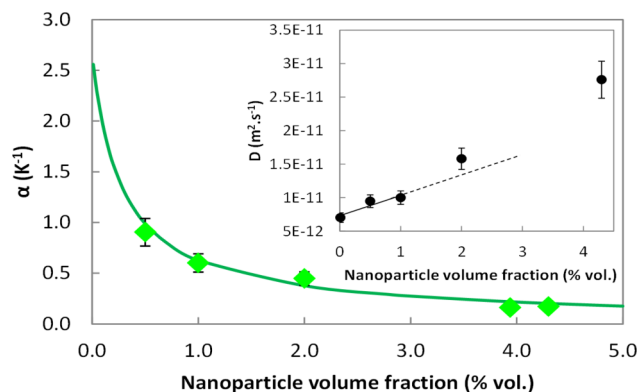

FIG. 1. Soret coefficient α and diffusion coefficient D (inset) as a function of NP volume fraction. Note that the measurements at higher concentrations ($\approx 4\%$) were performed on another set of DMSO based ferrofluids in similar ionic conditions.

extremities). The mean cell temperature was kept between 30 and 50 °C such that the coldest temperature in the cell stays well above the freezing point of DMSO 19 °C. The open circuit voltage is $\Delta V = -\Lambda \Delta T_{elect}$, where Λ shall be referred to as the "*thermoelectric coefficient*," to be distinguished from the Seebeck coefficient $\mathcal{S}_e$. The thermoelectric voltage was monitored over 2 h between each temperature change. The diffusion coefficient D (see inset in Figure 1) gives the nanoparticle diffusion time[26] $\tau = l^2/(\pi^2 D)$ of the order of two days for our thermocell. Thus, the observed electromotive force and thermoelectric coefficient Λ correspond to those of the "*initial state*"[4] (i.e., immediately after the onset of a temperature gradient while particle concentrations are uniform).

III. RESULTS AND DISCUSSION

A. Theoretical considerations

To analyse our experimental results, here we consider a colloidal solution containing a concentration n of charged particles with a structural diameter d and a structural charge Z_{str} (here, particles are positively charged). They are stabilized in a monovalent electrolyte solution A^+B^-. Some anions B^- are condensed within the first solvation layers of the particles, partly canceling Z_{str} thus leading to an effective charge $Z \ll Z_{str}$.[27] The remaining anions–whose Coulomb binding energy is smaller than $k_B T$–are free. The concentrations of free anions and cations are n_- and n_+, respectively. The electroneutrality writes

$$Zn + n_+ - n_- = 0. \tag{1}$$

Under a temperature gradient, the particle current $\boldsymbol{J}_i$ corresponding to the charged species i is[1,3]

$$\boldsymbol{J}_i = -D_i \left[\boldsymbol{\nabla} n_i + n_i \frac{\widehat{S}_i}{k_B T} \boldsymbol{\nabla} T - n_i \frac{\xi_i e}{k_B T} \boldsymbol{E} \right], \tag{2}$$

where n_i is the density of the ith species. The first term corresponds to Fick's diffusion with coefficient D_i, the second term is proportional to the "Eastman entropy of transfer," $\widehat{S}_i$, and the last term is the electric drift in the presence of a local field $\boldsymbol{E}$. It should be emphasized that here, the "Eastman

entropy of transfer", $\widehat{S}_i$ differs from the original definition given by Eastman;[28] rather, we follow the more generalized formalism of agar in which $\widehat{S}_i$ is understood from Onsager equations[4] (for more detail, see the supplementary material (Sec. II)[39]). $\widehat{S}_i = \overline{\overline{S}}_i - s_i$, where s_i represents the partial molar entropy and $\overline{\overline{S}}_i$ is the coefficient of the particle current $\boldsymbol{J}_i$ in the expression of the entropy current $\boldsymbol{J}_S = \sum_i \overline{\overline{S}}_i \boldsymbol{J}_i - \kappa \boldsymbol{\nabla T}/T$ (the second term is the Fourier contribution with heat conductivity κ). It is important to emphasize that $\widehat{S}_i$ makes no distinction among different interactions between the charged species and the surrounding solvent causing the thermal drift (i.e., electronic double layer (EDL), solvation effects, and osmotic pressure).

The dimensionless number $\xi_i = k_B T \mu_i^{el}/eD_i$ is proportional to the ratio of the electrophoretic mobility μ_i^{el} to the diffusion coefficient D_i.[3] For small point-like ions, the Einstein relation is valid and ξ_i is simply the ionic charge number z_i. The particle currents corresponding to small non-interacting monovalent ions are

$$\boldsymbol{J}_\pm = -D_\pm \left[\boldsymbol{\nabla} n_\pm + n_\pm \frac{\widehat{S}_\pm}{k_B T} \boldsymbol{\nabla T} \mp n_\pm \frac{e}{k_B T} \boldsymbol{E} \right]. \quad (3)$$

For colloidal particles, ξ is of the same order of magnitude as—but not equal to—the effective charge Z.[3] At large volume fractions, the interaction between NPs needs to be considered. This can be understood in terms of isothermal osmotic compressibility[5] between charged particles $\chi(\phi)$, where $\phi = V_{np} n$, with $V_{np} = \pi d^3/6$ the nanoparticle volume. The ϕ dependence of the parameters $\widehat{S}$ and ξ in Eq. (2) appears as

$$\widehat{S} = \widehat{S}_0 \chi(\phi)$$

and

$$\xi = \xi_0 \chi(\phi). \quad (4)$$

(For more information, please refer to the supplementary material (Sec. III).[39]) Choosing an effective hard sphere model with Carnahan-Starling equation of state,[29] $\chi(\phi)$ of charged particles becomes (see the supplementary material (Sec. III)[39])

$$\chi(\phi_{eff}) = \frac{(1 - \phi_{eff})^4}{1 + 4\phi_{eff} + 4\phi_{eff}^2 - 4\phi_{eff}^3 + \phi_{eff}^4}, \quad (5)$$

where $\phi_{eff} = \phi(d_{eff}/d)^3$ represents an effective volume fraction corresponding to the "effective" hard-sphere diameter $d_{eff} = d + 2\lambda_D$, with λ_D being the Debye length, and it corresponds also to the second coefficient $A_2 = 4(d_{eff}/d)^3$ of the virial development (as a function of ϕ of the osmotic pressure).[30]

When the stationary state (hereafter denoted by a superscript "*st*") is reached, each of the three currents expressed in Eqs. (2) and (3) vanishes. Combining these equations with the electroneutrality condition, Eq. (1), we obtain[1,3]

$$\boldsymbol{E}^{st} = \frac{1}{e} \left[\frac{Zn\widehat{S} + n_+ \widehat{S}_+ - n_- \widehat{S}_-}{n_+ + n_- + \xi Zn} \right] \boldsymbol{\nabla T} = \mathcal{S}_e^{st} \boldsymbol{\nabla T}. \quad (6)$$

Substituting this expression in the nanoparticle current Eq. (2), we obtain

$$\frac{\boldsymbol{\nabla} n}{n} = -\frac{1}{k_B T} (\widehat{S} - \xi e \mathcal{S}_e^{st}) \boldsymbol{\nabla T} = -\alpha \boldsymbol{\nabla T}, \quad (7)$$

where

$$\alpha = (\widehat{S} - \xi e \mathcal{S}_e^{st})/k_B T \quad (8)$$

is the Soret coefficient. For uncharged particles, only the first term is present. In a series of recent papers, Würger and coauthors[1,3,31,32] have emphasized the importance of the second term in charged colloidal suspensions. Recent experiments on the salinity (electrolytes) dependent thermodiffusion of polystyrene sulfonate beads[33] and of DNA molecules[34] appear to support these theoretical considerations.

B. Thermodiffusion and thermoelectric analysis

The Soret coefficient α, determined at different NP volume fractions ϕ is reported in Figure 1 with an inset showing the diffusion coefficient D. As can be seen from the figure, the initial linear regime of D extending up to $\phi = 1\%$ can be approximated by $D(\phi) \approx 7.32 \times 10^{-12}(1 + 41\phi)$ m^2 s^{-1}. The coefficient is indeed close to the $2 \times A_2 = 34.4$ value expected from the virial development (cf. the supplementary material (Sec. III)[39]). The overall behavior, i.e., the magnitude of the Soret coefficient and its dependence on NP concentration, is similar to those found in other ferrofluids (dispersed in water and/or kerosine). (See, for example, Refs. 22 and 35.) The variation in α was analyzed using Eqs. (6) and (8), with the approximation (to be justified later) $\widehat{S} >> \xi_0 \widehat{S}_+, \xi_0 \widehat{S}_-$, i.e.,

$$\alpha \approx \frac{1}{k_B T} \left[\frac{\widehat{S}(\phi_{eff})(1 + Z\tilde{n}/2)}{1 + (\xi(\phi_{eff}) + 1)Z\tilde{n}/2} \right]. \quad (9)$$

Here, we define $\tilde{n} = n/n^+$, where n^+ (H$^+$ ions) is kept constant. The nanoparticle structural diameter is $d = 6.7$ nm, the Debye length is $\lambda_D = 2.1$ nm in a solution of 12.5 mM HClO$_4$ in DMSO with dielectric constant $\epsilon = 48$ at room temperature, leading to $A_2 = 17.2$. $\xi_0 \approx 25$ was estimated from the measurement of the electrophoretic mobility of a NP suspension at $\phi = 0.05\%$ using the laser Doppler velocimetry technique (NanoZS Malvern GB). The remaining unknown parameters Z and $\widehat{S}_0$ are determined through the fit (solid line in Figure 1) of the experimental data by Eq. (9). We obtain $Z \approx 30(\pm 5)$ and $\widehat{S}_0 \approx 68(\pm 8)$ meV K^{-1}, or equivalently, $\widehat{S}_0/\xi_0 \approx 2.7$ meV K^{-1}, one order of magnitude higher than typical values corresponding to electrolytes,[4] which justifies our previous approximation, $\widehat{S} >> \xi_0 \widehat{S}_+, \xi_0 \widehat{S}_-$.

In thermoelectric measurements, a temperature gradient $\boldsymbol{\nabla T}$ is established across a previously isothermal, homogeneous electrolyte. While the bulk distribution of different species is still uniform, an internal electric field, $\boldsymbol{E}^{init}$, settles immediately within the fluid due to the charge accumulations at the cell boundaries arising from the mobility difference among different charged species.[4] This is due to the response of ions to thermal forces $\boldsymbol{f}_i = \widehat{S}_i \boldsymbol{\nabla T}$. In open circuit conditions, the total electric current $\boldsymbol{J}_{elec} = Ze\boldsymbol{J} + e\boldsymbol{J}_+ - e\boldsymbol{J}_-$ is zero. Substituting Eqs. (2) and (3) for the particle currents and taking into account the initial condition $\boldsymbol{\nabla} n_i = 0$, we obtain[4]

$$\boldsymbol{E}^{init} = \sum_i \frac{t_i \widehat{S}_i}{\xi_i e} \boldsymbol{\nabla T} = \mathcal{S}_e^{init} \boldsymbol{\nabla T}, \quad (10)$$

where $t_i = \sigma_i/\sigma_T$ is the Hittorf transport number of ionic species i, i.e., the relative contributions of its conductivity σ_i to the total conductivity, $\sigma_T = \sum_i \sigma_i$.

In a thermocell, where a reversible redox reaction occurs at the electrodes, the difference of electrochemical potential between the hot and the cold electrodes at initial state is $\Delta\tilde{\mu} = -e\Delta V^{init} = e\Lambda^{init}\Delta T$, with[4] (see the supplementary material (Sec. IV) for more detail[39])

$$\Lambda^{init} = \frac{\Delta s_r}{e} + \mathcal{S}_e^{init} = \frac{\Delta s_r}{e} + \sum_i \frac{t_i \widehat{S}_i}{\xi_i e}. \qquad (11)$$

The first term $\Delta s_r = s_{Fc^+} - s_{Fc}$ represents the redox reaction entropy at electrodes (i.e., the difference of the partial molar entropies of F_C^+ and F_C) which remains constant throughout the measurements. The second term arises from the initial electric field as described in Eq. (10).

The measured Λ^{init}, as a function of nanoparticle volume fraction (ϕ), at different temperatures, are shown in Figure 2. The measurements are repeated at least 5 times at each concentration and temperature. The data dispersion is less than 4%. The Λ^{init} values were found negative, as it can be expected from the negative redox reaction entropy of the F_C/F_C^+ couple,[36] and varied between -1.1 and -1.6 mV K^{-1}. The absolute value of Λ^{init} decreases with increasing ϕ as well as with the mean cell temperature.

At a fixed mean cell temperature and constant HClO$_4$ and F_C/F_C^+ concentrations, the variations in Λ^{init} stem from the term $t\widehat{S}(\phi)/(\xi(\phi)e)$ of NPs. The nanoparticles' contribution to the electrical conductivity: $\sigma = \xi(\phi)Ze^2nD(\phi)/k_BT$ is less than a few percent of the total conductivity σ_T at $\phi \leq 1\%$. The ϕ dependence of σ_T was thus neglected. Combined together, Eq. (11) can be rewritten as

$$\Lambda^{init}(\phi) = \Lambda^{init}(0) + \frac{Ze}{k_BT}\frac{\phi}{V_{np}}\frac{D(\phi)}{\sigma_T}\widehat{S}(\phi_{eff}). \qquad (12)$$

At room temperature, $D(\phi)$ is taken from the linear relation observed through forced Rayleigh scattering (Figure 1 inset). $\sigma_T = 35.5$ mS m^{-1} was measured at room temperature. Since the dominant temperature dependence of both D and σ_T arises from a same quantity, i.e., the inverse friction coefficient
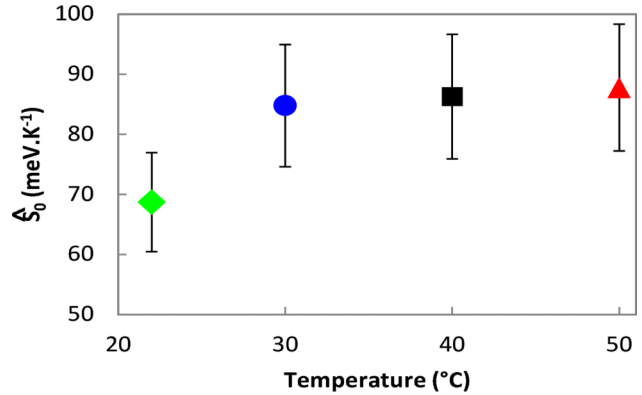
FIG. 3. Eastman transport entropy per NP in infinite dilution limit $\widehat{S}_0$ as a function of temperature, estimated by Seebeck (circle, square, and triangle) and Soret (diamond) coefficients based models. The large error bars are mainly due to the uncertainty in the average NP size ($\sigma = 0.38$).

$1/\eta(T)$ of the solvent, we shall take, as a first approximation, D/σ_T independent of T. The ϕ dependence of $\widehat{S}(\phi)$ is obtained from the effective hard sphere model (Eq. (4)). With $Z = 30$ and $d = 6.7$ nm, the experimental results (Figure 2) are fitted to Eq. (12) to deduce $\widehat{S}_0$. The results are compared in Figure 3 to the $\widehat{S}_0$ value determined from the forced Rayleigh scattering experiments at 23 °C. In the explored temperature range, $\widehat{S}_0$ determined from the Soret coefficient and the Seebeck coefficient measurements are ≈ 81.9 meV K^{-1}, i.e., three orders of magnitude higher than the "Eastman entropy of transfer" of small usual electrolyte ions (e.g., 0.12 meV K^{-1} for Na ions in water[4]) as expected for nanoparticles.

The origin of such a large value of $\widehat{S}_0$ is far from clear. $\widehat{S}_0$ includes all the individual contributions to the thermodynamical and transport properties of all species. For nanoparticles, it makes no distinction among different interactions between the charged species and the surrounding solvent causing the thermal drift (i.e., EDL and solvation effects). One most likely contribution is that of the EDL surrounding the charged nanoparticles, which results from the surrounding counter ions and the ionic strength of the solvent. Such an effect has been demonstrated to influence the thermodiffusive behavior of charged colloids[37] without taking in account the thermoelectric field across the solution. We have used existing theoretical models[32,38] to estimate the EDL contribution to the overall $\widehat{S}_0$ with $\lambda_D = 2.1$ nm, $d = 6.7$ nm, and the temperature dependent dielectric constant of DMSO. Our calculation yields $\widehat{S}_{EDL}$ of 6 meV K^{-1} or less, falling an order of magnitude short of the observed $\widehat{S}_0$, suggesting additional mechanisms at play. Defined as such,[4] $\widehat{S}_0$ encompasses all individual contributions to the thermodynamical and transport properties making no distinction among different interactions between nanoparticles and the surrounding solvent (i.e., EDL, solvation effects, and electrolyte salinity).

IV. CONCLUSION

In this work, we have measured the thermoelectric coefficient of an ionically stabilized ferrofluid as a function of nanoparticle volume fraction and compared the results to the corresponding Soret effect measurements. As expected,
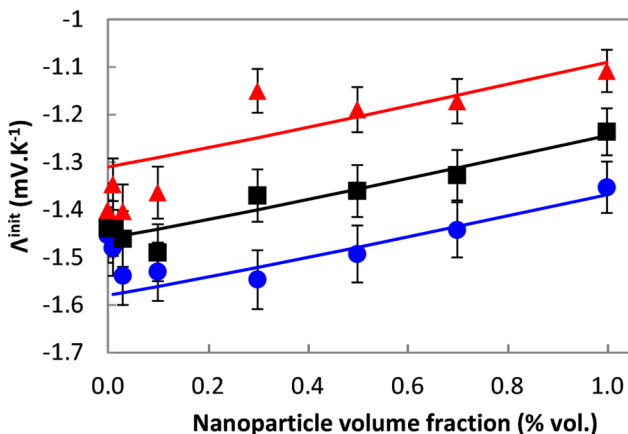

FIG. 2. Λ^{init} measured as a function of NP volume fraction ϕ at cell median temperatures of 30 (circles), 40 (squares), and 50 °C (triangles). The solid lines are fits to Eq. (12). See text for more explanation.

both coefficients depend on the concentration of charged nanoparticles, and the values of "Eastman entropy of transfer," $\widehat{S}_0$, determined from both experiments are found to be in fair quantitative agreement. Our results lend strong support to the existing theoretical models describing charged colloidal solutions' thermoelectric and thermodiffusive properties that both depend on $\widehat{S}_0$. Following the same rationale, one can postulate that the sign and the magnitude of Seebeck and Soret coefficients must depend on several experimental parameters, e.g., the relative importance of the "Eastman entropy of transfer" between nanoparticles and surrounding ions, the concentration of *all* charged species in the solution, and the surface charge of colloidal particles. These extensive parameters can be tuned experimentally to control the thermoelectric coefficient Λ of charged colloidal suspensions to test the validity of the current theoretical model. Simultaneously, the current finding offers a new perspective in future liquid thermocell research using charged colloids.

ACKNOWLEDGMENTS

[1]A. Würger, Phys. Rev. Lett. **101**, 108302 (2008).

[2]H. Sugioka, Langmuir **30**, 8621 (2014).

[3]A. Majee and A. Würger, Phys. Rev. E **83**, 061403 (2011).

[4]J. Agar, "Thermogalvanic cells," in *Advances in Electrochemistry and Electrochemical Engineering*, edited by P. Delahay (Interscience, New York, 1963), pp. 31–121.

[5]D. Vigolo, S. Buzzaccaro, and R. Piazza, Langmuir **26**, 7792 (2010).

[6]S. Putnam and D. Cahill, Langmuir **21**, 5317 (2005).

[7]Y. Marcus, Chem. Rev. **109**, 1346 (2009).

[8]H. Ning, S. Datta, T. Sottmann, and S. Wiegand, J. Phys. Chem. B **112**, 10927 (2008).

[9]H. Ning, J. Dhont, and S. Wiegand, Langmuir **24**, 2426 (2008).

[10]S. Duhr and D. Braun, Proc. Natl. Acad. Sci. U. S. A. **103**, 19678 (2006).

[11]D. Stadelmaier and W. Köhler, Macromolecules **42**, 9147 (2009).

[12]R. Piazza and A. Parola, J. Phys.: Condens. Matter **20**, 153102 (2008).

[13]T. Völker, E. Blums, and S. Odenbach, Int. J. Heat Mass Transfer **47**, 4315 (2004).

[14]P. Salazar, S. Stephens, A. Kazim, J. Pringle, and B. Cola, J. Mater. Chem. A **2**, 20676 (2014).

[15]L. Sprenger, A. Lange, and S. Odenbach, C. R. Mec. **341**, 429 (2013).

[16]G. K. E. Blums, V. Sints, and A. Mezulis, C. R. Mec. **341**, 348 (2013).

[17]L. Sprenger, A. Lange, and S. Odenbach, Phys. Fluids **26**, 022001 (2014).

[18]A. Gunawan, C. Lin, D. Buttry, V. Mujica, R. Taylor, R. Prasher, and P. Phelan, Nanoscale Microscale Thermophys. Eng. **17**, 304 (2013).

[19]*Magnetic Fluids and Applications Handbook*, edited by B. Berkovski (Begell House, Inc. Publishers, New York, 1996).

[20]R. Massart, IEEE Trans. Magn. **17**, 1247 (1981).

[21]I. Lucas, S. Durand-Vidal, E. Dubois, J. Chevalet, and P. Turq, J. Phys. Chem. C **111**, 18568 (2007).

[22]G. Demouchy, A. Mezulis, A. Bée, D. Talbot, J. Bacri, and A. Bourdon, J. Phys. D: Appl. Phys. **37**, 1417 (2004).

[23]A. Bacri, A. Bourdon, G. Demouchy, B. Heegaard, B. Kashevsky, and R. Perzynski, Phys. Rev. E **52**, 3936 (1995).

[24]V. Zinovyeva, S. Nakamae, M. Bonetti, and M. Roger, ChemElectroChem **1**, 426 (2014).

[25]M. Bonetti, S. Nakamae, M. Roger, and P. Guenoun, J. Chem. Phys. **134**, 114513 (2011).

[26]J. N. Agar and J. Turner, Proc. R. Soc. A **225**, 307 (1959).

[27]L. Belloni, Colloids Surf. **140**, 227 (1997).

[28]E. D. Eastman, J. Am. Chem. Soc. **50**, 283 (1928).

[29]N. Carnahan and K. Starling, J. Chem. Phys. **51**, 635 (1969).

[30]F. Cousin, E. Dubois, and V. Cabuil, Phys. Rev. E **68**, 021405 (2003).

[31]A. Würger, Langmuir **25**, 6696 (2009).

[32]S. Fayolle, T. Bickel, and A. Würger, Phys. Rev. E **77**, 041404 (2008).

[33]K. A. Eslahian, A. Majee, M. Maskos, and A. Würger, Soft Matter **10**, 1931 (2014).

[34]M. Reichl, M. Herzog, A. Götz, and D. Braun, Phys. Rev. Lett. **112**, 198101 (2014).

[35]L. Sprenger, A. Lange, Z. Yu, and S. Odenbach, Phys. Fluids **27**, 022001 (2015).

[36]J. Hupp and M. J. Weaver, Inorg. Chem. **23**, 3639 (1984).

[37]Z. Wang, H. Kriegs, J. Dhont, and S. Wiegand, Soft Matter **9**, 8697 (2013).

[38]J. Dhont, S. Wiegand, S. Duhr, and D. Braun, Langmuir **23**, 1674 (2007).

[39]See supplementary material at http://dx.doi.org/10.1063/1.4927665 for (I) cyclic voltammograms, (II) entropy of transfer, (III) hard core interactions, and (IV) initial thermoelectric coefficient.